J. COMBIN. MATH. COMBIN. COMPUT. 127b (2025) 9321--9335

Journal of Combinatorial Mathematics and Combinatorial Computing
www.combinatorialpress.com/jcmcc

Economic Behavior Modeling and Market Optimization Strategies Based on Game Theory and Deep Learning

Xinxin Chen[1], Jun Shao[1,✉]

[1] *School of Economic and Management, Southeast University, Nanjing, Jiangsu, 211189, China*

ABSTRACT

Grasping economic behavior is a foothold of market optimization, this paper combines game theory ideas with deep learning technology to explore the laws of economic behavior. Firstly, different payment strategies are considered and payment matrices are constructed, and replicated dynamic equations are used to describe the dynamic adjustment process of the game and simulate the game process of market economic transactions. The MS-RCNN model that can be used to predict economic behavior is constructed by extracting data features using CNN and processing the feature matrix using GRU. The results of the game simulation simulation show that when the government regulation of the market is in place, it is easier for the trading parties to reach a deal. In addition the MS-RCNN model can more accurately reflect the fluctuation of the market when making long-term and short-term predictions, and the predicted price is closer to the real market price. Therefore a better understanding of economic behavior through game theory and its prediction through deep learning helps to achieve the optimization of market strategies.

Keywords: game theory, deep learning, MS-RCNN, economic behavior modeling

1. Introduction

In the modern market economy, the government and the market together play a role in promoting the operation and development of the economy [1]. With the development of social economy, the government's economic behavior plays a more extensive positive role in the development of the economy [2]. Every major initiative of China's economic system reform is essentially an adjustment of the government's economic behavior. Clarifying the model of government economic behavior is the foundation and premise of studying government economic behavior [3-4].

There are two main modes of government economic behavior in the world, one is "development-oriented" and the other is "regulatory" [5]. The so-called "development-oriented" refers to the fact that the government puts the development of the economy in the first place, cultivates the market for this

✉ Corresponding author.
E-mail address: jj4202195@163.com (J. Shao).
Received 25 March 2024; Revised 05 June 2024; Accepted 15 December 2024; Published Online 16 April 2025.
DOI: 10.61091/jcmcc127b-510

purpose, utilizes the market, and plans, regulates and controls the economy [6]. Japan, the Four Little Dragons of Asia and a number of rising developing countries in East Asia have mostly opted for this type of governmental behavioral model [7]. The so-called “regulatory” means that the government focuses on regulating the market and maintains the market order by regulations, so as to make the economy operate and develop smoothly and rationally. This is the mode of government behavior in most developed countries [8-9]. As a developing country in transition to a market economy and moving towards industrial modernization, the “development-oriented” model should be the inevitable choice of the Government. That is to say, the orientation of the Chinese government's economic behavior must be development-oriented, to promote the sustained, healthy and rapid development of the national economy as its own basic principle and primary goal [10-12]. Whether the government intervenes in an economic activity, how it intervenes, and the intensity of its intervention are judged by whether it can effectively promote economic development [13]. For a large developing country like us, which is economically and culturally backward and in a period of institutional transition and catching up stage, accelerating development is the most urgent subject, “the key to solving all problems in China is to rely on its own development, and strive for a faster speed and higher efficiency” [14-15]. From an international perspective, the economic rise of Japan and the four Asian small dragons also owes much to the accelerated development of the economy, now, we have the domestic conditions, the international environment is conducive, coupled with the advantages of the socialist system can focus on doing big things, in the process of modernization and construction of the future, the emergence of a number of stages of development at a relatively fast pace, the efficiency of a relatively better, it is necessary, but also can be done [16-17].

On the other hand, understanding the reasons why local government economic behaviors may cause market segmentation is not the same as finding ways to directly break up market segmentation. Because these behaviors often involve specific environmental background and institutional basis, and the latter is constantly changing [18-19]. Among them, some changes will be in the process of the market economy's own development and improvement, for example, some backward areas of “local protectionism” tendency will be faded out as the level of development of the region [20]. Others can be adjusted in the process of technological progress, such as Internet trade to break the regional blockade, greatly reducing the possibility of market segmentation. Still others are objective facts that are difficult to change, and the inevitable mutual competition and corresponding interests of local governments in the process of economic development is a prominent point [21-22]. Especially in the unbalanced economic development between regions, it is more necessary to fully mobilize the enthusiasm of local governments to develop the regional economy.

Formulating economic policies and making decisions on major economic activities is itself an important economic behavior of the government. In order to make the government's decision-making effective rather than ineffective, and to have long-term utility rather than emergency action, it is necessary to set up a correct decision-making value goal and optimize the government's decision-making system [23-24]. Decision-making is a complex, finite-rational process. Decision-making behavioral process and its structure is only the decision-making process of “behavior” appearance, while the decision-making value judgment process and its structure, is the real core of decision-making. Therefore, establishing correct decision-making value objectives is the key to optimize government decision-making. Different decision-making value objectives will form different value orientation and evaluation standards of the decision-making process. Government decision-making should be in line with the practical needs and be able to solve the real problems as the value orientation, i.e., “applicable” as the value objective [25-26]. This requires the government in the formulation of a policy, or test and evaluation of a policy, should be based on whether the policy is in line with the situation at the time, to solve the real problem as the standard. After the reform and opening up, many economic decisions have been effective precisely because the government has implemented the value orientation of “applicability” in decision-making [27-28]. Game theory and deep learning have the advantage of being applied to modeling economic behavior, which can theoretically analyze the underlying logic of the government's economic behavior in a more objective and three-dimensional way.

In this paper, the economic behavior of the two parties to the transaction is assumed, and the payment matrix is constructed under different combinations of payment strategies. Based on this matrix, the dynamic adjustment process of strategy selection between the two parties of the game is described by replicating the dynamic equation, and the evolutionary stable strategy of the game is solved by using differential equations. An economic behavior prediction model is constructed based on deep learning to provide support for market strategy optimization. The reconstruction layer of the model generates multi-scale economic behavior data. The feature layer uses CNN to extract the features of the multi-scale data and outputs the feature map after convolution unit. The fusion layer uses GRU to process the feature matrix and measures the learning error of the model using cross entropy at the output layer. This paper also simulates the game process of economic behavior to test the market optimization effect of the economic prediction model.

2. Modeling economic behavior based on game theory

2.1. Basic assumptions

Economic behavior is a pattern of behavior in which goods are sold to different subjects. Merchants provide goods, and consumers choose to consume or not to consume the goods according to their personal situation, and need to pay consumption costs or bear other economic costs. Based on this, the article puts forward hypothesis 1: the two sides of the game for the demand side of the commodity (consumers) and the provider (merchants), their decision-making behavior are limited, rational, strategy selection interacts with each other, there is no isolated behavior, so consumers and merchants can choose the optimal game strategy according to their own situation. Hypothesis 2: In order to promote a more orderly and healthy development of the economy, the government will regulate it and play a great role, when the intensity of government regulation increases, the economy will be greatly affected, mainly affecting the provider of goods, i.e. merchants.

2.2. Construction of the payment matrix

There are differences in the payment levels of consumers and merchants under different combinations of strategies, while the payment matrix of the merchant-consumer game is as follows:

$$P_1 = \begin{cases} r_r - p_r \\ -L_r \\ -kc_m \\ -c_m \end{cases} \tag{1}$$

where: r_r represents the benefits that accrue to consumers when they choose to buy and use the commodity. p_r denotes the cost expenditure incurred by the consumer in choosing to purchase the use of the commodity. L_τ denotes the utility loss incurred by the consumer in the absence of the commodity available. k denotes the intensity of government regulation, which takes values ranging from 0 to 1, with the closer to 1 denoting the greater the intensity of regulation. c_m denotes the economic loss incurred by merchants who do not offer the good.

An analysis of the payment matrix reveals that $r_r - p_r$ is the payment made when a consumer chooses to purchase a good. -L_τ is the loss of utility incurred by the consumer when there is no good available, i.e., the negative payment when the purchase of the good does not provide a benefit. $-kc_m$ is the level of payment when the merchant offers the good and the consumer chooses to purchase an alternative, taking into account the total cost of purchasing an alternative and the cost to the merchant of offering the good and the impact of government regulation. $-c_m$ is the economic loss incurred when the merchant does not offer the good.

2.3. *Game Model Analysis*

Based on the payment matrix shown above, firstly, the replicated dynamic equations in the evolutionary game theory are used to portray the dynamic adjustment process of the strategy choices of the two sides of the game, so that u_1 represents the expected payment of the consumer choosing the purchase strategy, u_2 represents the expected payment of the consumer choosing the no-purchase strategy, and represents the average payment of the consumer. Next, consider a randomized pairwise game between multiple merchants and multiple consumers, assuming that the proportion of consumers choosing to purchase goods is x, and the proportion of consumers choosing not to purchase or purchasing goods on their own is $1-x$. The proportion of merchants choosing to provide goods is y, and the proportion of merchants choosing not to provide goods is $1-y$. Then, we have:

$$\begin{cases} u_I = y(r_r - p_r) + (l-y)(L_r) \\ u_2 = y(r_r - c_r \div n_r) + (l-y)(r_r - c_r \div n_r) \\ \bar{U} = xU_I + (l-y)U_2 \end{cases} \tag{2}$$

where: c_r denotes the total cost that the consumer spends if he/she chooses not to purchase the use of the good, and n_r denotes the maximum number of times the consumer can use the good if he/she has purchased a substitute for it.

According to the definition of the replication dynamic equation [29], the consumer's replication dynamic equation can be described by the following differential equation:

$$F(x) = \frac{d_x}{d} = x(U_1 - \bar{U}) = x(1-x)[y(r_r - p_r + L_r) - L_r - r_r + c_r \div n_r] \tag{3}$$

Therefore, the equation for the merchant's replication dynamics can be obtained as:

$$F(y) = \frac{d_x}{d_t} = y(1-y) = x\left[(p_r - \frac{c_r}{n_r}) - kc_r - c_n - c_m\right] \tag{4}$$

where: c_n denotes the equalized cost incurred by the merchant for managing the goods after providing them.

Joint equations (3) and (4) obtain a two-dimensional dynamic system, which describes the dynamic adjustment mechanism of the strategy selection of the two types of game groups, consumers and merchants, and then uses the stability theory of differential equations to solve the game's evolutionary stable strategy.

3. Deep learning-based economic behavior prediction models

3.1. *Problem definition*

In this paper, the economic behavior data are classified into different categories, and the data set is denoted as $\mathrm{D} = \{(x_i, y_i)\}_N$, where N is the number of samples in the dataset, $x_i \in \square^T$ is the i-moment sample with dimension T, and $y_i \in \square$ is the corresponding label. The input data can be denoted as $x_i = \{x_1, x_2, \cdots, x_\tau\}$, where x_j is the value of the jth moment counted from the starting moment, and T is the total length of each input data.

The learning objective of economic behavior prediction is to construct a nonlinear mapping function from input sequences x_i to category labels y_i:

$$y_i = f(x_i) \tag{5}$$

where $f(\cdot)$ is the nonlinear function to be learned.

The linear models used in traditional economic behavior analysis methods cannot capture this complex nonlinear relationship, so this paper proposes a multi-scale recurrent convolutional neural network (MS-RCNN) model. The model reconstructs the input single-scale data into multiscale data with several different scales, and then uses a deep learning-based model to sequentially extract features from each scale, fuse the multiscale data, and output the predicted categories.

3.2. *Model structure*

The model in this paper has four layers:

1) Reconstruction layer: reconstructs a single-scale input data into multi-scale data. Specifically, this layer obtains multiple different scales of data by subjecting the original input to multiple time-domain downsampling operations with different parameters.

2) Feature layer: uses independent convolutional units to extract features from the input data at different scales. The length of the output feature maps from the convolutional units dealing with different scales will be different, in order to facilitate the computation, this layer fills all the feature maps to the same length and then stitches them together.

3) Fusion Layer: this layer employs a family of RNN models to better capture the highly nonlinear correlation and complementarity of features at different scales to obtain features that fuse multi-scale data.

4) Output Layer: this layer consists of two layers of fully connected network, which inputs the fused multi-scale features and outputs the final classification result of the model.

3.2.1. Reconfiguration layer. Assume an input sequence $x = \{x_1, x_2, \cdots, x_T\}$ with a time-domain downsampling rate of d_o. This means that every d momentary data point in the original data is extracted for generating data $x^d = \{x_d, x_{2d}, \cdots, x_{md}\}$ with scale d, where $m = T / ds$ is the length of the sequence x^d. With this method, multiple data with different scales can be generated, e.g., $s = 1, 2, \cdots, d$ can generate data $\{x^1, x^2, \cdots, x^d\}$ with corresponding scales, denoted using X.

3.2.2. Feature layer. The feature layer takes multi-scale data as input and outputs the features extracted from each scale of data. This layer has two main basic units: the convolutional network unit and the splicing operation unit.

The basic component of this unit is the Convolutional Neural Network (CNN). The CNN is chosen as a feature extractor to extract features from data at different scales. Specifically, the convolutional network unit uses independent one-dimensional convolutional networks (1dCNN) to process the data at each different scale [30]. These 1dCNNs have the same settings for feature template size and number of templates.

The original sequence is first reconstructed into multiple different scales of data using time-domain downsampling, and then the features are extracted using a convolutional network, similar to the features extracted by combining different levels of hijacking in an image. Second, multiscale convolution can obtain longer-term trend features in larger scale data than the original scale data, combining multiple scales and thus obtaining trend information that encompasses different time spans. In addition, the extension of multiscale convolution on time scales is obtained by downsampling the input data instead of increasing the filter size, which can reduce the amount of computation to some extent.

Let x^d denote the data generated by d-scale temporal downsampling, and the weights $w_j^d \in \mathbb{R}^k$ of the corresponding convolutional network are used to extract features from this data. Here, k is the window size. c_{ij}^d The computational formula is as follows:

$$c_{i,j}^d = f_a(w_j^d * x_{i:i+k-1}^d + b_j^i) \tag{6}$$

In the above equation, $*$ denotes the convolution operation, $b_j^i \in \mathbb{R}$ is a bias term, and $f_a(\cdot)$ is a nonlinear function such as a modified linear unit (ReLU). The convolutional network will process the data $x^d = \{x_{1:k}^d, x_{2:k+1}^d, \cdots, x_{m-k+1:m}^d\}$ to obtain the feature map $c_{ij}^d \in \mathbb{R}^{m-k+1}$, which is calculated as follows:

$$c_j^d = \{c_{j,1}^d, c_{j,2}^d, \cdots, c_{j,m-k+1}^d\} \tag{7}$$

The splicing unit splices the feature maps output from CNNs at different scales in chronological order and fills them to the same length before splicing.

The length of the feature map decreases with the increase of the downsampling scale, in order to facilitate the calculation, here the feature maps obtained from different scale sequences through the convolution unit are filled to the same length. For example, for $d = 1$, the length of the feature map obtained by the convolution unit is $T - k + 1$. Here, the length of the feature maps obtained by the convolution unit for other scale sequences is filled to $T - k + 1$ by padding with zeros. To fill the feature maps obtained by the convolution unit for a d-scale sequence, the following operation is performed:

$$a_j^d = [z_1, z_2, \cdots z_{T-m}, c_{j,1}^d, c_{j,2}^d, \cdots, c_{j,m-k+1}^d] \tag{8}$$

where $a_j^d \in \mathbb{R}^{T-k+1}$ is the filled feature map generated by the jnd convolutional template for scales d and $z_1, z_2, \cdots z_{T-m}$, and the original feature map is of length $T - m$.

Next, the filled feature maps are spliced into a feature matrix. The formula for the splicing process is described as follows:

$$E = [a_1^1, a_2^1, \cdots, a_l^1, \cdots, a_1^d, a_2^d, \cdots, a_l^d]^T \tag{9}$$

where $E \in \mathbb{R}^{(d \times l) \times (T-k+1)}$ is the feature matrix of length $T - k + 1$ and l is the number of convolutional templates. The computational complexity of this layer of operation is $O((m - k + 1)^2 \times k^2 \times l)$.

3.2.3. Fusion Layer. The input to the fusion layer is the feature matrix E of the output of the feature layer, and the output is the trend category of the next moment of the original sequence y_t. The outputs of the feature layer, $E = \{e_1, e_2, \ldots, e_{T-k+1}\}$, $e_i \in \mathbb{R}^{d \times l}$, are similar to the vector matrix of a sentence transformed into word vectors in natural language processing. The goal of the fusion layer is to establish the trend category probabilities for the first t moments of the feature case at the next $t+1$ moments $p(y_t \mid e_1, e_2, \ldots, e_{T-k+1})$. To take full advantage of the complex relationships between these features, an RNN family of models is used to process the feature matrix E. The output of the fusion layer is the trend category probabilities for the next moments of the original sequence.

In this paper, GRU is used to process the feature matrix. Each recurrent unit of the gated recurrent unit (GRU) can adaptively capture complementarities at different time scales [31]. The hidden state at the moment of a given eigenvector e_i, ith can be calculated by the following equation:

$$h_i = f_{en}(e_i, h_{i-1}; \theta_{en}) \tag{10}$$

where $h_i \in \mathbb{R}^q$ is the hidden state of the GRU at moment i, q is the size of the hidden state, $e_i \in \mathbb{R}^d \times l$ is the ith column in the matrix E, $f_{en}(\cdot)$ is a nonlinear function, and θ_{en} is the parameter of the GRU.The output of the GRU is $h_{T-k+1} \in \mathbb{R}^q$, which can also be viewed as a multiscale encoding of the input sequence. The computational complexity of this layer is $O((T-k+1)\times\theta_{en})$.

3.2.4. Output layer. The multi-scale codes output from the GRU are transformed by the nonlinear transformation of the fully connected layer and then fed into the softmax layer to obtain the probability distributions of the different classes. The softmax activation function is computed as follows:

$$p_i' = \frac{e^{o_i}}{\sum_C e^{o_j}} \tag{11}$$

where denotes the result of the i st output node and C denotes the number of categories. In order to learn the parameters of each layer, the cross-entropy is used here to measure the learning error of the model. Specifically, the cross-entropy loss function is used here to calculate the difference between the model's predicted categorization distribution and the actual categorization distribution, which is calculated as follows:

$$J_\theta = \frac{1}{N}\sum_{t=1}^{N}\sum_{j=1}^{C} p_{t,i}\log(p_{t,i}') \tag{12}$$

where θ represents all the parameters of the model and N is the total number of samples. Although the model is divided into multiple levels, the parameters of the model can be learned end-to-end.

4. Game behavior simulation and market strategy optimization

4.1. Simulation of the behavior of the economic game

Matlab 2018 is utilized to carry out simulation operations. In order to test the influence of government regulation on the behavioral choices of economic agents, it is assumed that k may take three values, namely, k=0, k=0.3 and k=1. The corresponding x_e^* in the corresponding case is calculated to be 0.15, 0.225, 0.4, and y_e^* to be 0.9225, respectively.

The following simulates, one by one, the evolution of the strategy choices of the two game parties when the initial choices of the two types of game groups are located in the regions Ⅰ, Ⅱ, Ⅲ and Ⅳ defined in the previous section, respectively.

The initial choices of the two types of game groups are located in region I, i.e., $x(0) < x_e^*$, $y(0) < y_e^*$, and this situation corresponds to the situation where the proportion of consumer groups choosing to purchase and use the goods at the beginning of the game is less than x_e^*, and the proportion of merchant groups choosing to provide the sharing strategy is less than y_e^*. Figure 1 shows the evolutionary dynamics of the game for initial states (0.1, 0.2), (0.3, 0.4) and (0.9, 0.6).

From Figure 1, we can see that the final evolutionary results are consistent with the theoretical analysis, in different initial states, the game eventually converges to the evolutionary stable strategy $x^* = 0$ and $y^* = 0$, the final evolutionary stable state for the consumer chooses not to buy and use the goods, and the businessman chooses not to provide the goods. At the same time, from Figure 1, we can also find that at this time, the government's regulatory policy no longer affects the final evolution of the game's stable state, but different regulatory intensity, the evolution time of the game to the stable state of the main body of the game is slightly different, which can probably be explained by the fact that in this case, both the consumer and the businessman do not have enough knowledge of the economy, and the willingness to participate in the economy is not high, so that the government's regulation can not play a big role.

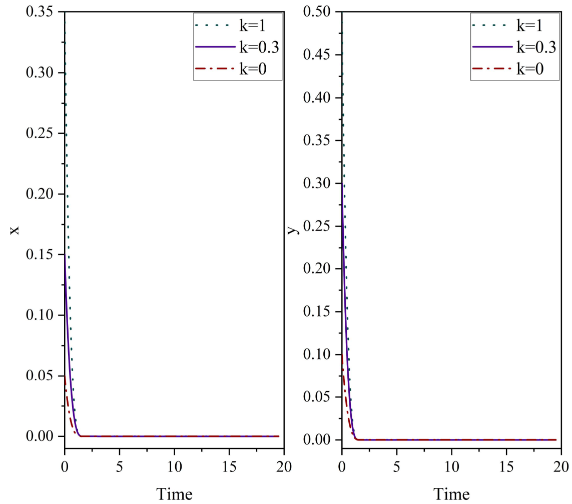

Fig. 1. The game evolution of the different initial states

The initial choices of the two types of game groups are located in region II, i.e., $x(0) > x_e^*$, $y(0) > y_e^*$, which corresponds to the situation where the proportion of consumers choosing to purchase and use the goods is greater than x_e^*, and the proportion of merchants choosing to provide the sharing strategy is greater than y_e^* at the beginning of the game. Figure 2 shows the evolutionary dynamics of the game for initial states (0.25, 0.96), (0.55, 0.98) and (0.85, 0.98).

Under different initial states, the game eventually converges to the evolutionary stable strategies $x^*=1$ and $y^*=1$, and the final evolutionary stable state is that consumers choose to buy and use the goods and merchants choose to provide the goods. At the same time, Figure 2 also reveals that the government's regulatory policy affects the time course of the game's evolution to the stable state, and when the government's regulation is more stringent, the game's subject will evolve more quickly to the final stable state, which may be explained by the fact that in this case, consumers and merchants have clear understanding of the economy, and the willingness to participate in the economy is higher, and the government's high-intensity regulation at this time serves as the icing on the cake. This may be explained by the higher willingness of both consumers and businesses to participate in the economy in this scenario, and the icing on the cake of intense government regulation.

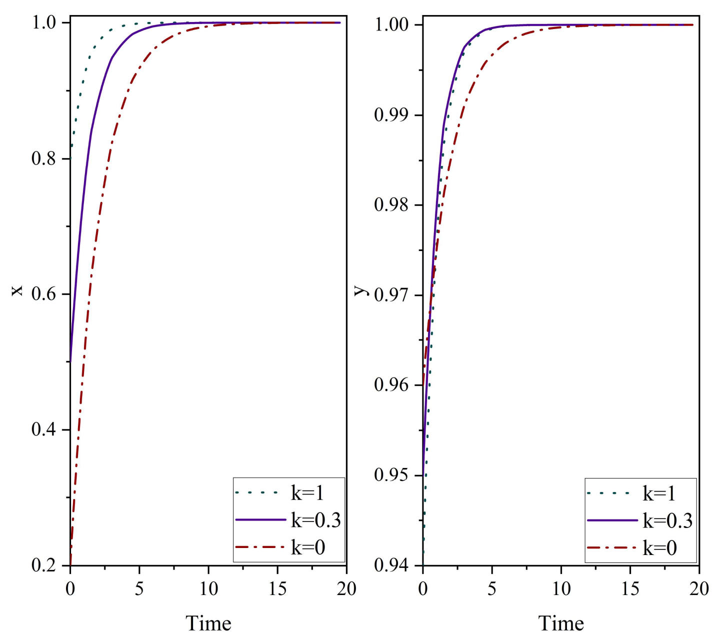

Fig. 2. The game evolution of the different initial states

The initial choices of the two types of game groups are located in region III, i.e., $x(0) < x_e^*$, $y(0) > y_e^*$, and this scenario corresponds to the situation where the proportion of consumer groups choosing to purchase and use the goods at the beginning of the game is less than x_e^*, and the proportion of merchant groups choosing to provide the sharing strategy is greater than y_e^*. Figure 3 shows the evolutionary dynamics of the game when the initial states are (0.25, 0.95), (0.55, 0.96) and (0.85, 0.98).

Under different initial states, the game may eventually converge either to the evolutionary stable strategies $x^*=0$ and $y^*=0$ or to the evolutionary stable strategies $x^*=1$ and $y^*=1$. It can also be found that the government's regulatory policy affects the direction of the game's eventual evolutionary stable states, and when the government regulation is sufficiently strong (for the case with k=1), the game evolves to the stable states $x^*=1$ and $y^*=1$. When government regulation is not strong enough (for cases with k = 0 and k = 0.3), the game evolves towards the steady states $x^*=0$ and $y^*=0$. This may be explained by the fact that in this case the merchants have a clearer understanding of the economy while the consumers do not have a clearer understanding of the economy, and thus the strong government regulation promotes a larger proportion of merchants to adopt the strategy of providing the goods, and the consumers can consume the goods more conveniently in their lives, so that more and more consumers are willing to choose to buy and use the goods, and eventually evolve to the stable states $x^*=1$ and $y^*=1$.

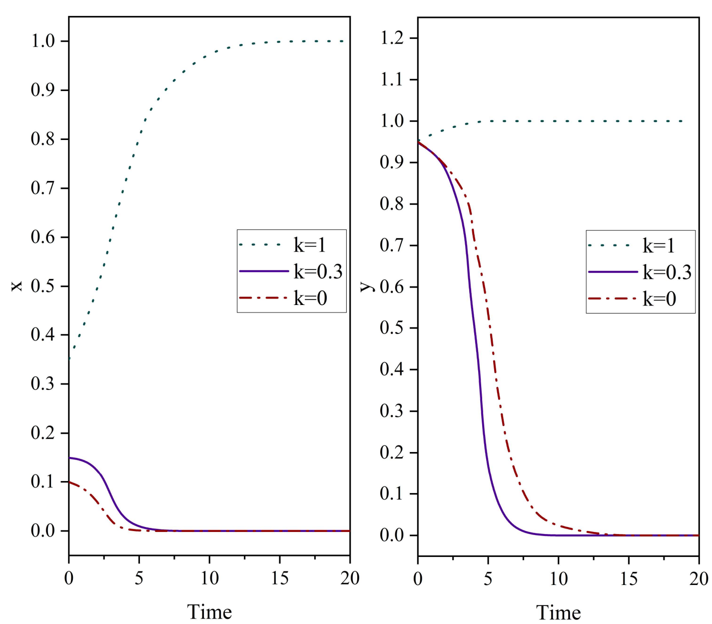

Fig. 3. The game evolution of the different initial states

The initial choices of the two types of game groups are located in region IV, i.e., $x(0) > x_e^*$, $y(0) < y_e^*$, and this scenario corresponds to the situation where the proportion of the consumer group choosing to purchase and use the goods is greater than x_e^* at the beginning of the game, and the proportion of the merchant group choosing to provide the sharing strategy is less than y_e^*. Figure 4 shows the evolutionary dynamics of the game for the initial states (0.25, 0.6), (0.55, 0.7) and (0.85, 0.85).

The evolution results of the game are similar to Figure 3, in that under different initial states, the game eventually converges to two stable states, one is $x^*=0$ and $y^*=0$, and the other is $x^*=1$ and $y^*=1$. The specific state to which the game converges is regulated by the government regulatory policy, and when the government regulation is sufficiently strong (for the case with k = 1), the game evolves to the stable states $x^*=1$ and $y^*=1$. When government regulation is insufficient (for the cases with k

= 0 and k = 0.3), the game evolves to the steady states $x^*=0$ and $y^*=0$, and this result can be interpreted similarly to the previous case.

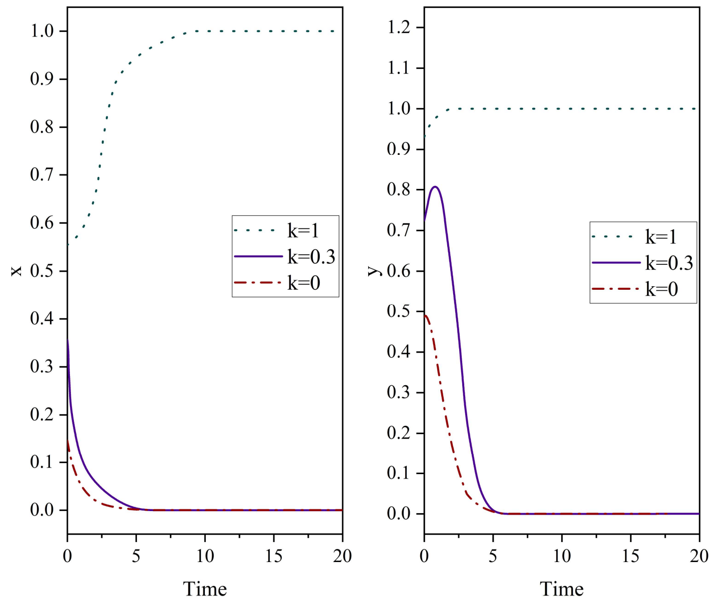

Fig. 4. The game evolution of the different initial states

4.2. Market strategy optimization effects

In this paper, we use Python deep learning software to forecast the long and short-term futures prices of six non-ferrous metals, aluminum, copper, nickel, lead, tin and zinc, from SHFE and LME, respectively. In view of this paper for a variety of non-ferrous metals to predict the effect of research, the relative error index is selected as the prediction evaluation index. In this paper, the average absolute percentage error (MAPE) is chosen, and the smaller the MAPE value is, the higher the prediction accuracy and the better the prediction effect of the model.

4.2.1. Comparison of long-term forecasting effects. In this paper, a time length of 250 trading days is chosen to measure the long-term prediction results of the MLP model, the LSTM model, and the MS-RCNN model for the closing prices of non-ferrous metal futures. Table 1 and 2 show the prediction results for aluminum, copper, nickel, lead, tin, and zinc traded on SHFE and LME.

Comparing the observations horizontally, for both SHFE and LME, the MAPE values of the LSTM model are smaller than those of the MLP model in the long-term forecasts of the six non-ferrous metal futures. Meanwhile, the MAPE values of the MS-RCNN model for the price forecasts of the six non-ferrous metal futures are again smaller than the MAPE values under the LSTM model. The results illustrate that the LSTM, MLP and MS-RCNN models have the highest prediction accuracy of the MS-RCNN linear model, followed by the LSTM model, and lastly by the MLP model, in the long-term prediction of SHFE and LME.

Table 1. The SHFE long-term prediction of nonferrous futures

Nonferrous metal	MAPE		
	MLP	LSTM	MS-RCNN
Aluminum	1.63	0.67	0.60
Copper	2.28	1.01	0.70
Nickel	8.71	2.10	1.29
Lead	1.28	1.05	0.75
Tin	3.74	1.42	0.94
Zinc	1.29	0.78	0.77

Table 2. The LME long-term prediction of nonferrous futures

Nonferrous metal	MAPE		
	MLP	LSTM	MS-RCNN
Aluminum	1.96	0.89	0.73
Copper	2.77	1.10	0.85
Nickel	2.90	1.48	1.39
Lead	1.57	1.04	1.01
Tin	2.25	1.43	1.00
Zinc	1.81	1.51	1.06

Figure 5(a), (b) and (c) shows the price charts of SHFE futures copper under the long-term forecasts of the MLP model, the LSTM model and the MS-RCNN model, which can more clearly and intuitively see the forecasting effect of each model. Combining the 2 metal futures markets, it can be concluded that in the long-term prediction, the prediction effect of the MS-RCNN model on the prices of the 6 non-ferrous metals is better than that of the LSTM model as a whole, and the prediction effect of the MLP model is the least satisfactory.

Longitudinal comparison of observed data: for LME forecasts, due to the earlier origin of the UK futures market, the futures contracts for each metal are listed and traded earlier, so the data are more adequate, and the forecasts of futures prices for the six non-ferrous metals do not show any anomalies. For SHFE forecasts, the MLP model, LSTM model and MS-RCNN model all show large deviations in the forecasts of nickel and tin at the same time, and the deviations of the MLP model and LSTM model are particularly obvious, with the MAPE values of nickel being 8.71, 2.10 and 1.29 respectively, and the MAPE values of tin being 3.74, 1.42 and 1.00, which is the highest of the MAPE values of each of the models in the six non-ferrous metal futures. 2 groups with the largest MAPE values for each model among the non-ferrous metal futures. The main reason for such great instability in the prediction is that the futures contracts of nickel and tin were only officially listed on SHFE on March 25, 2023, so there are fewer trading data and fewer training sets for the two, resulting in a great limitation in the training process of the nonlinear model MLP and LSTM, and the prediction model will end before the convergence effect, so there are very large fluctuations in the prediction process, and the prediction effect is not good.

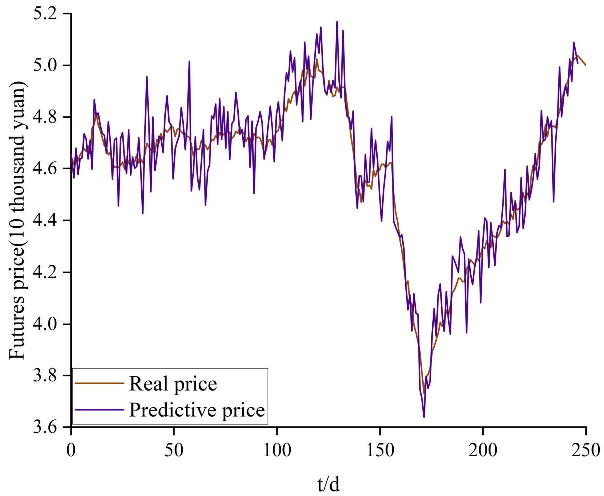

(a) MLP model

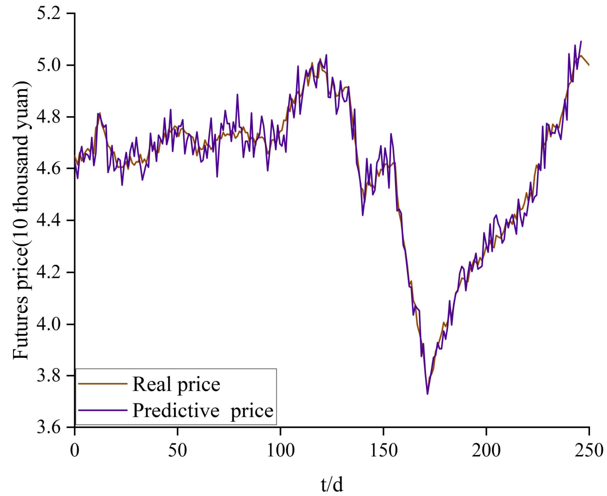

(b) LSTM model

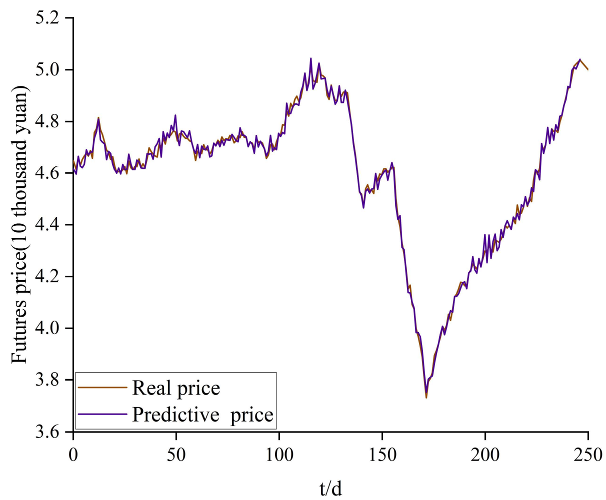

(c) MS-RCNN model

Fig. 5. The price trend of SHFE futures copper in the long term

4.2.2. Comparison of short-term forecasting effects. In this paper, a time length of 20 trading days is chosen to measure the short-term forecasts of the MLP, LSTM and MS-RCNN models for the closing prices of non-ferrous metal futures. Tables 3 and 4 show the prediction results for aluminum, copper, nickel, lead, tin and zinc traded on SHFE and LME.

In the short-term prediction of the closing prices of six non-ferrous metal futures, the MAPE values of the SHFE and LSTM neural network models are smaller than those of the MLP model except for the non-ferrous metal nickel. For 3 nonferrous metals, aluminum, lead and zinc, the MAPE values of LSTM model are slightly larger than those of MS-RCNN model. For 2 nonferrous metals, nickel and tin, the LSTM model MAPE values are more different from the MS-RCNN model. For the nonferrous metal copper, the LSTM model MAPE values are slightly smaller than the MS-RCNN model. Therefore, the accuracy of short-term forecasting of non-ferrous metal futures traded in SHFE using MS-RCNN linear is better, the LSTM model is slightly inferior, and the MLP model is not as effective.

Table 3. The SHFE short-term prediction of nonferrous futures

Nonferrous metal	MAPE

	MLP	LSTM	MS-RCNN
Aluminum	1.01	0.39	0.32
Copper	1.48	0.53	0.55
Nickel	2.52	2.64	1.01
Lead	4.57	0.90	0.72
Tin	2.51	1.74	0.80
Zinc	0.95	0.70	0.70

For the short-term prediction of the closing prices of six non-ferrous metal futures on the LME, the MAPE values of the LSTM neural network model are smaller than those of the MLP model. Meanwhile, it can be found that the MAPE values of LSTM neural network models for 4 non-ferrous metal futures, aluminum, nickel, tin and zinc, are larger than those of MS-RCNN model, which indicates that 4 non-ferrous metal futures, aluminum, nickel, tin, and zinc, which are traded in LME, are better predicted by using MS-RCNN linear model. The MAPE value of the LSTM model for 2 non-ferrous metals, copper and lead, is smaller than that of the MS-RCNN model, indicating that the LSTM model performs better in these 2 futures varieties. It can be concluded that in short-term forecasting, the overall effect of the MLP model is not satisfactory enough, but the prediction accuracy of the LSTM model and the MS-RCNN model are comparable.

Table 4. The LME short-term prediction of nonferrous futures

Nonferrous metal	MAPE		
	MLP	LSTM	MS-RCNN
Aluminum	2.34	0.61	0.64
Copper	2.13	0.74	0.78
Nickel	2.92	1.85	1.04
Lead	1.72	1.12	1.13
Tin	1.47	1.20	0.74
Zinc	1.93	1.32	0.81

5. Conclusion

In this paper, the payment matrix construction and game model analysis of market economic behavior are carried out, and the economic behavior prediction model is designed by using deep learning technology.

The game process of economic behavior is simulated, and it is found that the strength of government regulation affects the evolution time and direction of the game. When government regulation is strong enough, i.e., consumers choose to buy and use goods, and merchants choose to provide goods. When government regulation is not strong enough, consumers tend to choose not to buy and use the goods, and merchants choose not to provide the goods. This indicates that effective government regulation and the improvement of laws and regulations have an important impact on market economic behavior. Compared with LSTM and MLP, the MS-RCNN model in this paper has better long- and short-term prediction effects for both LME trading and SHFE trading markets, achieves smaller MAPE results, and its predicted prices are more closely fitted to the real market prices.

Therefore, this paper achieves realistic simulation and accurate prediction of economic behavior based on game theory and deep learning, which is conducive to further deepening the understanding of economic behavior by each trading party, so as to optimize the market strategy in a targeted way.

References

[1] Bursztyn, L., & Jensen, R. (2017). Social image and economic behavior in the field: Identifying, understanding, and shaping social pressure. Annual Review of Economics, 9(1), 131-153.

[2] Tresch, R. W. (2022). Public finance: A normative theory. Academic Press.

[3] Wright, A. L., Sonin, K., Driscoll, J., & Wilson, J. (2020). Poverty and economic dislocation reduce compliance with COVID-19 shelter-in-place protocols. Journal of Economic Behavior & Organization, 180, 544-554.

[4] Chen, W., & Hu, Z. H. (2018). Using evolutionary game theory to study governments and manufacturers' behavioral strategies under various carbon taxes and subsidies. Journal of Cleaner Production, 201, 123-141.

[5] Ashraf, B. N. (2020). Economic impact of government interventions during the COVID-19 pandemic: International evidence from financial markets. Journal of behavioral and experimental finance, 27, 100371.

[6] Wilkinson, N., & Klaes, M. (2017). An introduction to behavioral economics. Bloomsbury Publishing.

[7] Antulov-Fantulin, N., Lagravinese, R., & Resce, G. (2021). Predicting bankruptcy of local government: A machine learning approach. Journal of Economic Behavior & Organization, 183, 681-699.

[8] Grimmelikhuijsen, S., Jilke, S., Olsen, A. L., & Tummers, L. (2017). Behavioral public administration: Combining insights from public administration and psychology. Public Administration Review, 77(1), 45-56.

[9] McConnell, C., Margalit, Y., Malhotra, N., & Levendusky, M. (2018). The economic consequences of partisanship in a polarized era. American Journal of Political Science, 62(1), 5-18.

[10] Ramey, V. A., & Zubairy, S. (2018). Government spending multipliers in good times and in bad: evidence from US historical data. Journal of political economy, 126(2), 850-901.

[11] Benartzi, S., Beshears, J., Milkman, K. L., Sunstein, C. R., Thaler, R. H., Shankar, M., ... & Galing, S. (2017). Should governments invest more in nudging?. Psychological science, 28(8), 1041-1055.

[12] Colantone, I., & Stanig, P. (2018). The trade origins of economic nationalism: Import competition and voting behavior in Western Europe. American Journal of Political Science, 62(4), 936-953.

[13] Viscusi, W. K., Harrington Jr, J. E., & Sappington, D. E. (2018). Economics of regulation and antitrust. MIT press.

[14] Kremer, M., Rao, G., & Schilbach, F. (2019). Behavioral development economics. In Handbook of behavioral economics: applications and foundations 1 (Vol. 2, pp. 345-458). North-Holland.

[15] Leenders, R. (2017). Spoils of truce: Corruption and state-building in postwar Lebanon. Cornell University Press.

[16] Silva, P. C., Batista, P. V., Lima, H. S., Alves, M. A., Guimarães, F. G., & Silva, R. C. (2020). COVID-ABS: An agent-based model of COVID-19 epidemic to simulate health and economic effects of social distancing interventions. Chaos, Solitons & Fractals, 139, 110088.

[17] Blazquez, D., & Domenech, J. (2018). Big Data sources and methods for social and economic analyses. Technological Forecasting and Social Change, 130, 99-113.

[18] Hazen, B. T., Mollenkopf, D. A., & Wang, Y. (2017). Remanufacturing for the circular economy: An examination of consumer switching behavior. Business Strategy and the Environment, 26(4), 451-464.

[19] Gale, W. G., & Samwick, A. A. (2017). Effects of income tax changes on economic growth. The economics of tax policy, 13-39.

[20] Shiller, R. J. (2020). Narrative economics: How stories go viral and drive major economic events. Princeton University Press.

[21] Hughes-Cromwick, E., & Coronado, J. (2019). The value of US government data to US business decisions. Journal of Economic Perspectives, 33(1), 131-146.

[22] Chen, X., Cao, J., & Kumar, S. (2021). Government regulation and enterprise decision in China remanufacturing industry: Evidence from evolutionary game theory. Energy, Ecology and Environment, 6, 148-159.

[23] Jones, L. P., & Sakong, I. (2020). Government, business, and entrepreneurship in economic development: The Korean case (Vol. 91). BRILL.

[24] Liu, Y., Quan, B. T., Xu, Q., & Forrest, J. Y. L. (2019). Corporate social responsibility and decision analysis in a supply chain through government subsidy. Journal of cleaner production, 208, 436-447.

[25] Deming, W. E. (2018). The new economics for industry, government, education. MIT press.

[26] Colander, D. C. (2017). Economics. McGraw-Hill.

[27] Al-Thaqeb, S. A., & Algharabali, B. G. (2019). Economic policy uncertainty: A literature review. The Journal of Economic Asymmetries, 20, e00133.

[28] Nugent, N. (2017). The government and politics of the European Union. Bloomsbury Publishing.

[29] Zhang Ying & Zhu Haojie. (2022). Stochastic Evolutionary Game in Food Takeaway Management with Improved Replication Dynamic Equations in Postepidemic Era. Mathematical Problems in Engineering.

[30] Pengfei Pang,Jian Tang(Member CCF),Ting Rui,Jiancheng Gong & Yuchen He. (2024). Research on fault diagnosis and feature extraction mechanism visualization of rotating machinery based on improved 1D CNN. Advances in Mechanical Engineering(10).

[31] Xinhui Kang,Ying Luo,Qi Zhu & Can Wu. (2025). Research on Kansei design of electric scooter integrating CNN-GRU-Attention and biologically inspired design. Expert Systems With Applications 126121-126121.